

Evolution of deformation in the neutron-rich krypton isotopes: The ^{96}Kr nucleus

N. Mărginean,¹ D. Bucurescu,^{1,2} C. A. Ur,^{1,3} C. Mihai,¹ L. Corradi,⁴ E. Farnea,³ D. Filipescu,¹ E. Fioretto,⁴ D. Ghiță,¹ B. Guiot,⁴ M. Górska,⁵ M. Ionescu-Bujor,¹ A. Iordăchescu,¹ D. Jelavić-Malenica,⁶ S. M. Lenzi,³ P. Mason,³ R. Mărginean,¹ D. Mengoni,⁴ G. Montagnoli,³ D. R. Napoli,⁴ S. Pascu,¹ G. Pollarolo,⁷ F. Recchia,⁴ A. M. Stefanini,⁴ R. Silvestri,⁴ T. Sava,¹ F. Scarlassara,³ S. Szilner,⁶ and N. V. Zamfir¹

¹Horia Hulubei National Institute of Physics and Nuclear Engineering, R-76900 Bucharest, Romania

²Academy of Romanian Scientists, 54 Splaiul Independenței, R-050094 Bucharest, Romania

³Istituto Nazionale di Fisica Nucleare, Sezione di Padova, I-35131 Padova, Italy

⁴INFN-Laboratori Nazionali di Legnaro, I-35020 Legnaro, Italy

⁵Gesellschaft für Schwerionenforschung (GSI) D-64291 Darmstadt, Germany

⁶Ruder Bošković Institute, Zagreb, Croatia

⁷Dipartimento di Fisica and INFN, I-10125 Torino, Italy

(Received 12 June 2009; published 5 August 2009)

The energy of the first excited 2^+ state in ^{96}Kr was measured as 241 keV. The nucleus was produced in the fission of ^{238}U induced by a 954-MeV ^{136}Xe beam and prompt γ rays were observed using the clover array CLARA in coincidence with fission products identified with the PRISMA spectrometer. The evolution of the quadrupole collectivity in the Kr isotopes with $N \geq 50$ is discussed by comparison with that from the Rb to Mo isotones and with predictions of various theoretical calculations.

DOI: [10.1103/PhysRevC.80.021301](https://doi.org/10.1103/PhysRevC.80.021301)

PACS number(s): 21.10.Re, 23.20.Lv, 27.60.+j

Introduction. The outstanding interest in studying the neutron-rich nuclei with mass $A \approx 100$ dates back to the first theoretical prediction of large deformation of the ground states in nuclei around ^{100}Zr [1] and its experimental confirmation [2]. In this region, with $Z \approx 40$ and $N > 56$, the ground-state properties were found to depend very sensitively on small changes in both Z and N , giving rise to different structure phenomena such as shape coexistence, large variations of the quadrupole collectivity, low-lying intruder states, and octupole correlations, with a rich literature addressing these problems as early as 1988 [3]. Especially striking among these phenomena has been the observation of a sudden onset of large quadrupole deformation in the Sr and Zr isotopes, which takes place around $N = 60$: $N = 58$ isotopes are quasispherical, while the $N = 60$ ones are rigid rotors with a large deformation, close to $\beta_2 = 0.40$, see e.g. Refs. [4,5] and references quoted therein. Many theoretical calculations were devoted to the explanation of this phenomenon. Microscopically, it was found [6] that this onset of deformation can be associated with a sudden decrease, at $N = 60$, of the occupancy of the proton orbital $1f_{5/2}$ and of the neutron $2d_{5/2}$ and $1g_{9/2}$ orbitals, accompanied by a substantial increase of the occupancy of the proton $1g_{9/2}$ and neutron $1h_{11/2}$ orbitals; to this, one adds a certain effect of the strong interaction between the particles occupying the spin-orbit partner orbitals proton $1g_{9/2}$ and neutron $1g_{7/2}$, a mechanism earlier invoked by Federman and Pittel [7]. There are also many mean-field-based calculations of the equilibrium deformation and moments at low spins, potential energy surfaces, shape coexistence, and shape transitions in this region (see Ref. [4] and the many references quoted there). They all show that the strong shape variations in this region are due to shell effects associated with spherical and deformed gaps in the single-particle spectrum: spherical gaps due to shell and subshell closures at $Z = 38, 40$ and $N = 56$, and deformed

ones at $|\beta_2| \approx 0.35$ at $Z = 36, 38, 40$ and $N = 60, 62, 64$. Most of these calculations provide large deformations in Sr, Zr, and Mo isotopes with $N \geq 60$. The details of the shape transition around $N = 58$ are, nevertheless, different for the various models.

The nuclei of interest here are rather neutron-rich and are therefore difficult to access for spectroscopic study. Their ground-state properties are accessible via mainly two experimental ways: γ -ray spectroscopy studies of fission products or reaction fragments, or of their β decay (level schemes, level lifetimes), and laser spectroscopy studies (spins, moments, changes in the mean-square charge radii of isotopes).

Experimental information on the neutron-rich Krypton isotopes became available later than that for the Sr, Zr, and Mo isotopes. The first spectroscopic study of ^{92}Kr was reported in Ref. [8], while that for ^{94}Kr was given in Ref. [9] (together with a systematics of the properties of $^{88-94}\text{Kr}$). Laser spectroscopy measurements for ^{72}Kr to ^{96}Kr were reported by Ref. [10,11] and compared to previous similar measurements for the Sr isotopes [12,13]. For $N > 50$, except for ^{86}Kr , the $B(E2)$ electromagnetic transition probability for the $2_1^+ \rightarrow 0_{g.s.}^+$ transition was measured very recently by Coulomb excitation only for ^{88}Kr and ^{92}Kr [14]. No information on excited levels in ^{96}Kr existed until now.

Theoretically, there are many different predictions about the ground-state properties of the neutron-rich Kr nuclei. First potential energy surface (PES) calculations with the macroscopic-microscopic (Nilsson-Strutinsky) method were presented in Ref. [15] and predicted that ^{96}Kr is the first isotope expected with a large (oblate) deformation of $\beta_2 \approx 0.30$. Other calculations are those with the finite-range droplet model (FRDM) with both the early [16] and more refined [17] versions of the model, the extended Thomas-Fermi

with Strutinsky integral (ETFISI) model [18], the relativistic mean-field model (RMF) [19], and the Nilsson-Strutinsky calculations with a Woods-Saxon potential [4]. The results of these calculations will be discussed in the last part of this article.

One should mention also the great interest for the properties of the heavy Kr isotopes (with $A \geq 96$) that were proposed as waiting-point nuclei in certain scenarios of the rapid neutron-capture process (*r*-process) [20,21].

In the present communication we report a first spectroscopic investigation of the ^{96}Kr nucleus, which provided the excitation energy of its first excited 2^+ state. After presenting the experimental approach and its result, the implications of this experimental value for the evolution of the nuclear deformation along the neutron-rich Kr isotopic chain will be discussed.

Experimental. Neutron-rich nuclei in the Zn-Pd region were produced in the transfer reactions and Coulomb-induced fission of ^{238}U , produced by bombarding it with ^{136}Xe beam. The ^{136}Xe beam was delivered by the PIAVE-ALPI complex at INFN—Laboratori Nazionali di Legnaro (Italy); it was produced by the electron cyclotron resonance source of PIAVE, preaccelerated, injected in the ALPI booster, and accelerated to 954 MeV. The target consisted of a 1 mg/cm² metallic ^{238}U foil supported on both sides by 10–45 $\mu\text{g}/\text{cm}^2$ carbon foils. Following the bombardment of ^{238}U with ^{136}Xe a multitude of isotopes were produced in processes like quasielastic, deep-inelastic, quasifission, or induced fission of ^{238}U . The reaction products were detected and identified using the large-acceptance magnetic spectrometer PRISMA [22] placed at 54° with respect to the beam direction. The spatial

coordinates at the entrance in the spectrometer were measured with the MCP start detector of PRISMA, the same detector giving also the start for the measurement of time of flight inside the spectrometer. The ions then passed through two magnetic elements, one quadrupole lens set to vertical focus and horizontal dispersion and a 1-m-wide dipole. The coordinates of the ion trajectories in the focal plane and the stop signal for the time of flight were obtained using a 1-m-wide multiwire PPAC detector segmented in 10 transversal sections. Subsequently, the ions were stopped in a 10×4 section segmented ionization chamber that provided partial energy releases in the sections transited by each ion and made possible the identification of its atomic number and total kinetic energy. The trajectories inside the spectrometer were reconstructed in the off-line analysis, finally leading to unambiguous identification of mass, Z , charge state and velocity vector for every ion detected with PRISMA. Mass resolution achieved was $A/\Delta A \approx 200$ for masses ranging from 70 to 140 and Z resolution was 1/60, allowing clear identification of elements from Zn to Cs. Gamma rays promptly emitted by reaction products in the target position were detected with the clover array CLARA [23] used in coincidence with PRISMA. Doppler correction of γ energies was performed in an event-by-event basis using the velocity vector measured with PRISMA, the energy resolution obtained being $\sim 0.8\%$.

Figure 1 shows γ -ray spectra gated by the isotopic peaks (in PRISMA matrices) of ^{96}Kr and of its isotones ^{98}Sr and ^{100}Zr . While for the Sr and Zr isotones we clearly observe the known first three transitions of the ground state band, only one weak peak is observed in the ^{96}Kr spectrum. γ rays from the fission

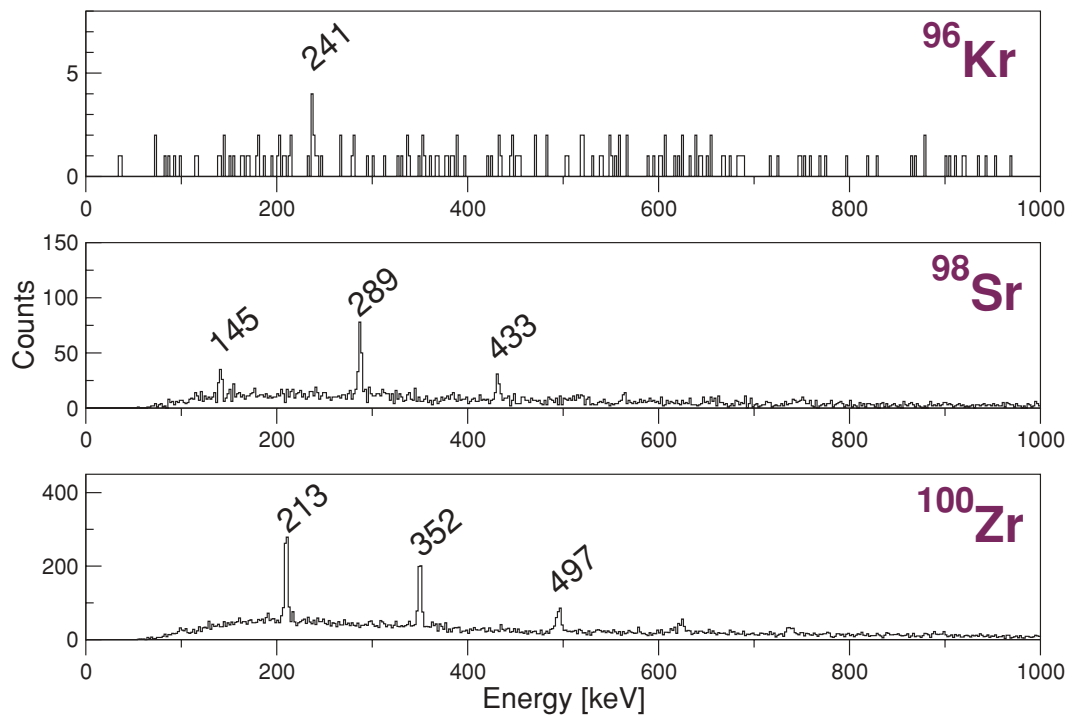


FIG. 1. (Color online) Gamma-ray spectra of $N = 60$ isotones, as obtained in the induced fission of ^{238}U . The spectra were obtained with the CLARA γ -ray array, and were gated by the specified isotopes, detected and identified with the PRISMA spectrometer. The presented spectra have 2 keV per channel.

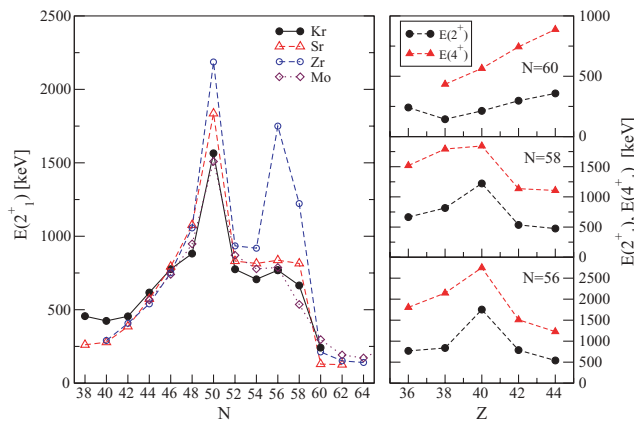


FIG. 2. (Color online) Systematics of the $E(2_1^+)$ values in different isotopic chains in the $A \approx 100$ region (left), as well as of the $E(2_1^+)$ and $E(4_1^+)$ energies as a function of Z for Kr, Sr, Zr, Mo (right).

partners are not seen in these spectra because the performed Doppler correction spreads them very much in energy. The 241-keV γ ray from the ^{96}Kr spectrum has been assigned to the $2_1^+ \rightarrow 0_{g.s.}^+$ transition in this nucleus. This assignment is not so straightforward. Figure 2 shows the evolution of the energy of the excited 2_1^+ state along isotopic chains, as well as that of the energies of the 2_1^+ and 4_1^+ states with the Z number from Kr to Mo. On the basis of the evolution of $E(4_1^+)$ for the $N = 60$ isotones, one could argue that the 241-keV γ ray in ^{96}Kr might be the $4^+ \rightarrow 2^+$ transition; in this case, the $2^+ \rightarrow 0^+$ transition would have an energy in the region from 103 keV (if this nucleus is a perfect rotor) to ~ 160 keV [if it has an $E(4^+)/E(2^+)$ ratio of about 2.5], and its absence from the spectrum in Fig. 1 appears to correlate with the strong suppression of the 145 keV $2^+ \rightarrow 0^+$ transition of ^{98}Sr (we note, however, that the 145-keV transition is weak not only because of the detection efficiency but also due to the 2.8-ns half-life of the 2^+ state). This solution, solely based on the extrapolation of the energy of the $4^+ \rightarrow 2^+$ transition is, nevertheless, difficult to support. First, extrapolating in such a region of sudden changes is dangerous; such an energy for the 2_1^+ state would be one of the lowest known in the region, indicating a rather large deformation (and therefore a very sudden structure change). Second, if we look at the behavior in the $N = 58$ and $N = 56$ isotones, one can see that the trend of the Kr isotopes is similar to that of the Mo isotopes, which, applied to $N = 60$, recommends the assignment of the 241-keV γ ray to the 2^+ state. Third, as it will be discussed below, both experimental laser spectroscopy results and all existing theoretical predictions for ^{96}Kr indicate a moderate deformation, which roughly corresponds to this value for the 2^+ state energy. We thus prefer this later assignment, but it remains as a task of future $\gamma\gamma$ -coincidence spectroscopy to prove that.

Discussion. In Fig. 2 one can see the well-known sudden decrease of the 2^+ state energy in the Sr and Zr isotopes, from $N = 58$ to $N = 60$. In the Mo isotopes, this quantity is almost constant between $N = 52$ and 56 , and then there is a smooth decrease for higher N . In the Kr isotopes, the decrease of $E(2_1^+)$ from $N = 56$ to 58 is smaller, and then it drops

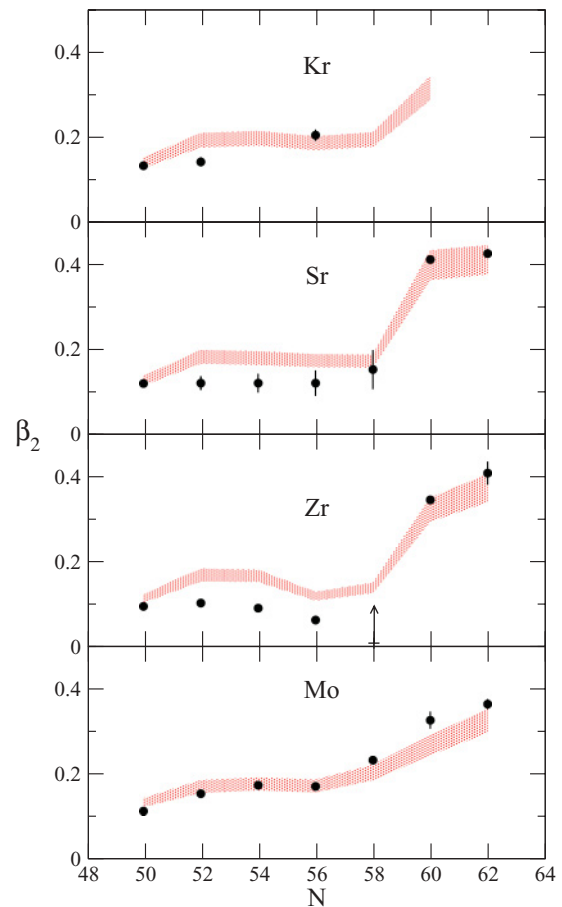


FIG. 3. (Color online) Quadrupole deformation β_2 values in the neutron-rich Kr, Sr, and Zr isotopes. The black circles are values deduced from the experimental $B(E2; 2_1^+ \rightarrow 0_{g.s.}^+)$ values (from Ref. [14] for ^{88}Kr and ^{92}Kr , and Ref. [24] for the rest of the nuclei). The hatched area is the domain predicted by the empirical formula of Raman *et al.* [25], given in the text.

from 666 keV at $N = 58$ to 241 keV at $N = 60$. Although this decrease is not as large as those observed for Sr and Zr, it may indicate a relatively large change of deformation between $N = 58$ and $N = 60$. We discuss the possible features of this transition by comparison with the Sr and Zr isotopes and with the predictions of different theoretical calculations.

In Fig. 3 the quadrupole deformations β_2 of the Kr, Sr, Zr, and Mo nuclei with $N \geq 50$ are shown. The experimental β_2 values (symbols) were deduced from the known reduced transition probabilities $B(E2; 2_1^+ \rightarrow 0_{g.s.}^+)$ from the ENSDF database [24]. In the same figure are also shown the values calculated with Raman's formula [25] that empirically relates β_2 to the 2_1^+ level energy:

$$\beta_2 = (466 \pm 41)E(2_1^+)^{-1/2}A^{-1}.$$

This formula provides values about 10% lower than those given by the empirical formula of Grodzins [26].

In the Sr and Zr isotopes the sudden transition from quasispherical nuclei with $\beta_2 \sim 0.10$ for $N \leq 58$ to well-deformed nuclei ($\beta_2 \sim 0.40$) for $N \geq 60$ is obvious. One should observe that in both these two cases the Raman's

formula predicts too high values for the “spherical” ($N = 50$ – 58) nuclei (up to a factor of about 2) but works rather well for the deformed cases. In the Mo isotopes the deformation has a much smoother variation, the nuclei showing a significant deformation before the place of the sudden shape change. In Kr the situation is not equally clear because there are not many experimental determinations of the deformation [from $B(E2)$ values]. Similarly to Mo, it seems that at $N = 56$ the Kr nuclei reach a deformation of about 0.20. According to the values extracted with Raman’s formula, the deformation remains practically the same at $N = 58$ and then at $N = 60$ jumps to 0.31. Thus, the situation for Kr seems to be intermediate between that of Mo (smooth variation of the deformation) and that of Sr-Zr (sudden onset of the deformation).

It is interesting to compare the picture of the deformation evolution that was discussed above with results of the laser-spectroscopy experiments, where the relative variation of the mean-square charge radii, $\delta\langle r^2 \rangle$, is measured along isotopic chains: Kr [11], Rb [27], Sr [12,13], Y [28], Zr [29], and Mo [30] (the later reference shows the systematics of this quantity for all isotopic chains from Kr to Mo). All isotopes of Kr with mass from 72 to 96 were measured in Ref. [11]. For the isotopic chains of Rb to Zr (we discuss here only the neutron-rich isotopes, $N > 50$) this quantity shows a sudden increase at $N = 60$ that can be related to a sudden increase of the deformation (e.g., from β_2 of about 0.25 in ^{99}Zr to almost 0.40 in ^{100}Zr). In both Kr and Mo chains, $\delta\langle r^2 \rangle$ varies smoothly with the neutron number N , and this can be related to a smooth variation of the deformation for N approaching 60 [11,30]. For the Kr chain this conclusion is slightly different from that emerging from nuclear spectroscopy data [like $B(E2)$ values and 2_1^+ state energies, Fig. 3]. To understand this difference, one must examine the procedure used to estimate the deformation from the mean-square charge radii. In the laser spectroscopy experiments the usual procedure is to use the droplet model, with deformations calculated either from $B(E2)$ values, or from $E(2^+)$ values, to predict the variation of the mean-square charge radii. This procedure reproduces only qualitatively both the sudden increase observed in the case of Sr (it systematically underestimates $\delta\langle r^2 \rangle$ for 90 – ^{96}Sr), and the experimental results for Kr [11]. The differences between the mean-square charge radii measured from laser spectroscopy and those deduced from $B(E2)$ values are difficult to understand even on the basis of theoretical models more elaborated than the droplet model (which, with just one shape parameter, is not a good approximation for near-spherical nuclei). Other effects that could explain these differences were considered, outside the quadrupole deformation itself, such as possible octupole correlations [31], or small variations of the skin thickness [32].

Figure 4 presents a comparison of the experimental deformation values with those predicted by different model calculations. The Nilsson-Strutinsky calculations of Ref. [15] predict that for mass 88 to 92 the Kr isotopes are spherical, mass 94 is a soft, quasispherical nucleus, with a tendency toward deformation, while the mass 96 Kr is a well-deformed nucleus, with $\beta_2 \approx 0.3$ (oblate), which shows also a secondary prolate minimum with about the same deformation. A similar

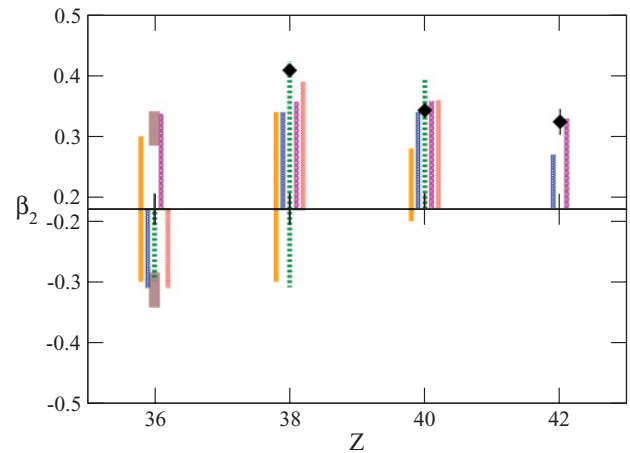


FIG. 4. (Color online) Comparison of experimental and theoretically predicted quadrupole deformations in the $N = 60$ Kr, Sr, Zr, and Mo isotones. For ^{96}Kr the experimental deformation (the hatched rectangle) is the value calculated with the Raman’s formula. For each isotone we represent the predictions of five theoretical calculations, drawn as sticks at the abscissas $Z - 0.2$, $Z - 0.1$, \dots , $Z + 0.2$, corresponding, respectively, to the following references: [4,15] (Nilsson-Strutinsky), [19] (RMF), [17] (FRDM), [18] (ETF-SI). When there was a strong prolate-oblate competition the solutions of both signs are represented (this is notably the case of Kr).

oblate deformation is provided by the analog calculations of Ref. [4]. Added to these two predictions we show the results of other three approaches: the extended Thomas-Fermi model with Strutinsky integral [18], the finite-range droplet model [17], and the relativistic mean-field model [19]. One can observe that all these calculations describe reasonably well the observed evolution. For the $N = 60$ Sr and Zr nuclei, most calculations predict prolate shapes. For ^{96}Kr , the magnitude of the deformation is predicted around 0.3, as the present experimental data suggest, most of the calculations (and notably, the relativistic mean field [19]) predicting an oblate deformation. Thus, the existing theoretical calculations appear to agree, at least qualitatively, with the picture we have now from the experimental data (Fig. 3), with small differences concerning the detailed mode in which the transition from $N = 58$ to $N = 60$ takes place. One should emphasize, nevertheless, that the RMF calculations are the only ones that describe reasonably well both the deformation data and the isotope shift data [11,19].

In conclusion, we measured the energy of the 2_1^+ excited state of ^{96}Kr , extending the empirical systematics, from nuclear spectroscopy data, of the evolution of the collectivity in the neutron-rich Kr isotopes. This enables a better comparison with other isotopic chains, of the behavior at the “deformation changing” $N = 60$ region. A sharp transition (or sudden onset of deformation) at this point takes place in the isotopic chains from Rb ($Z = 37$) to Zr ($Z = 40$), with the maximum variation in the Y chain ($Z = 39$) [30]. In Mo ($Z = 42$), the region $N = 50$ – 60 shows a gradual change of the deformation [30]. In the Kr chain ($Z = 36$), symmetrically placed to Mo with

respect to the center ($Z = 39$) of this region, the present data indicate that there may still be a relatively important change of deformation between $N = 58$ and $N = 60$, less drastic, however, than the corresponding transition in the isotonic Sr and Zr chains (Fig. 3). For a solid confirmation, and a more detailed comparison with different theoretical model predictions, measurements of the $B(E2)$ transition probability in both ^{94}Kr and ^{96}Kr , now possible by Coulomb excitations experiments, are highly desirable. Of high interest is also the experimental determination of the sign of the deformation,

which is also possible, in principle, by reorientation effects in Coulomb excitation.

We are grateful to the staff of the Tandem-ALPI accelerators of LNL for the excellent technical support. This work was supported by the European Community FP6—Structuring the ERA-Integrated Infrastructure Initiative—Contract EURONS No. RII3-CT-2004-506065 and partly by the Romanian Ministry for Education and Research under the CNCSIS Project Nos. ID-118 and ID-180.

-
- [1] D. A. Arseniev, A. Sobiczewski, and V. A. Soloviev, Nucl. Phys. **A139**, 269 (1969).
- [2] E. Cheifetz, R. C. Jared, S. G. Thompson, and J. B. Wilhelm, Phys. Rev. Lett. **25**, 38 (1970).
- [3] J. Eberth, R. A. Meyer, and K. Sistemich (eds.), *Nuclear Structure of the Zirconium Region* (Springer, Berlin, 1988).
- [4] J. Skalski, S. Mizutori, and W. Nazarewicz, Nucl. Phys. **A617**, 282 (1997).
- [5] W. Urban, J. L. Durell, A. G. Smith, W. R. Philips, M. A. Jones, B. J. Varley, T. Rzača-Urban, I. Ahmad, L. R. Morss, M. Bentaleb, and N. Schulz, Nucl. Phys. **A689**, 605 (2001).
- [6] A. Kumar and M. R. Gunye, Phys. Rev. C **32**, 2116 (1985).
- [7] P. Federman and S. Pittel, Phys. Lett. **B69**, 385 (1977); **B77**, 29 (1978); Phys. Rev. C **20**, 820 (1979).
- [8] K.-L. Kratz, H. Gabelmann, B. Pfeiffer, P. Möller, and (ISOLDE Collaboration), Z. Phys. A **330**, 229 (1988).
- [9] T. Rzača-Urban, W. Urban, A. Kaczor, J. L. Durell, M. J. Leddy, M. A. Jones, W. R. Phillips, A. G. Smith, B. J. Varley, I. Ahmad, L. R. Morss, M. Bentaleb, E. Lubkiewicz, and N. Schulz, Eur. Phys. J. A **9**, 165 (2000).
- [10] P. Lievens, E. Arnold, W. Borchers, U. Georg, M. Keim, A. Klein, R. Neugart, L. Vermeeren, and R. E. Silverans, Europhys. Lett. **33**, 11 (1996).
- [11] M. Keim, E. Arnold, W. Borchers, U. Georg, A. Klein, R. Neugart, L. Vermeeren, R. E. Silverans, and P. Lievens, Nucl. Phys. **A586**, 219 (1995).
- [12] F. Buchinger, E. B. Ramsay, E. Arnold, W. Neu, R. Neugart, K. Wendt, R. E. Silverans, P. Lievens, L. Vermeeren, D. Berdichevsky, R. Fleming, D. W. L. Sprung, and G. Ulm, Phys. Rev. C **41**, 2883 (1990).
- [13] P. Lievens, L. Vermeeren, R. E. Silverans, E. Arnold, R. Neugart, K. Wendt, and F. Buchinger, Phys. Rev. C **46**, 797 (1992).
- [14] D. Mücher, J. Iwanicki, A. Blazhev, P. Van Duppen, C. Fransen, J. Jolie, A. Linnemann, J. Mierzejewski, I. Ștefănescu, J. Van de Walle, N. Warr, K. Wrzosek, and (the MINIBALL Collaboration), Prog. Part. Nucl. Phys. **59**, 361 (2007).
- [15] D. Bucurescu, G. Constantinescu, D. Cutoiu, M. Ivașcu, and N. V. Zamfir, J. Phys. G **7**, L123 (1981).
- [16] P. Möller and J. R. Nix, At. Data Nucl. Data Tables **26**, 165 (1981).
- [17] P. Möller, J. R. Nix, W. D. Myers, and W. J. Swiatecki, At. Data Nucl. Data Tables **59**, 185 (1995).
- [18] Y. Aboussir, J. M. Pearson, A. K. Dutta, and F. Tondeur, Nucl. Phys. **A549**, 155 (1992).
- [19] G. A. Lalazissis and M. M. Sharma, Nucl. Phys. **A586**, 201 (1995).
- [20] U. C. Bergmann, C. Aa. Diget, K. Riisager, L. Weissman, G. Auböck, J. Cederkäll, L. M. Fraile, H. O. U. Fynbo, H. Gausemel, H. Jepsen, U. Köster, K.-L. Kratz, P. Möller, T. Nilsson, B. Pfeiffer, H. Simon, K. Van de Vel, J. Äusto, and (ISOLDE Collaboration), Nucl. Phys. **A714**, 21 (2003).
- [21] P. Delahaye, G. Audi, K. Blaum, F. Carrel, S. George, F. Herfurth, A. Herlert, A. Kellerbauer, H.-J. Kluge, D. Lunney, L. Schweikhard, and C. Yazidjian, Phys. Rev. C **74**, 034331 (2006).
- [22] A. M. Stefanini, M. Trotta, L. Corradi, A. M. Vinodkumar, F. Scarlassara, G. Montagnoli, and S. Beghini, Nucl. Phys. **A701**, 217c (2002).
- [23] A. Gadea *et al.* (the EUROBALL and PRISMA-2 Collaborations), Eur. Phys. J. A **20**, 193 (2004).
- [24] The ENSDF database, evaluated and maintained by the Brookhaven National Laboratory (www.nndc.bnl.gov/ensdf).
- [25] S. Raman, C. W. Nestor, Jr., and P. Tikkanen, At. Data Nucl. Data Tables **78**, 1 (2001).
- [26] L. Grodzins, Phys. Lett. **2**, 88 (1962).
- [27] C. Thibault, F. Touchard, S. Büttgenbach, R. Klapisch, M. de Saint Simon, H. T. Duong, P. Jacquinet, P. Juncar, S. Liberman, P. Pillet, J. Pinard, J. L. Vialle, A. Pesnelle, and G. Huber, Phys. Rev. C **23**, 2720 (1981).
- [28] B. Cheal, M. D. Gardner, M. Avgoulea, J. Billowes, M. L. Bissell, P. Campbell, T. Eronen, K. T. Flanagan, D. H. Forest, J. Huikari, A. Jokinen, B. A. Marsh, I. D. Moore, A. Nieminen, H. Penttila, S. Rinta-Antila, B. Tordoff, G. Tungate, and J. Äystö, Phys. Lett. **B645**, 133 (2007).
- [29] P. Campbell *et al.*, Phys. Rev. Lett. **89**, 082501 (2002).
- [30] F. C. Charlwood *et al.*, Phys. Lett. **B674**, 23 (2009).
- [31] H. Mach, F. K. Wohn, G. Molnár, K. Sistemich, J. K. Hill, M. Moszyński, R. L. Gill, W. Krips, and D. S. Brenner, Nucl. Phys. **A523**, 197 (1991).
- [32] F. Buchinger, R. Corriveau, E. B. Ramsay, D. Berdichevsky, and D. W. L. Sprung, Phys. Rev. C **32**, 2058 (1985).